Construction of the FORS Focal Reducer/Spectrographs: Status report and first test results

H. Nicklas
University Observatory Göttingen, Geismarlandstr. 11
D-37083 Göttingen, Germany

W. Seifert
Landessternwarte Heidelberg, Königstuhl
D-69117 Heidelberg, Germany

H. Böhnhardt, S. Kiesewetter-Köbinger
University Observatory München, Scheinerstr. 1
D-81679 München, Germany

G. Rupprecht
European Southern Observatory, Karl-Schwarzschild-Str. 2
D-85748 Garching, Germany

ABSTRACT

The hardware construction of FORS1, the first of the two focal reducer/low dispersion spectrographs of the ESO Very Large Telescope (VLT), is now finished. An extensive testing programme is under way which will guarantee that the instrument is fully understood and well calibrated when it will be installed at the Cassegrain focus of the first Unit Telescope of the VLT in 1998. This programme includes a full characterization of the optical system and the evaluation of the setting accuracies and reproducibility of the numerous electromechanical functions as well as testing the flexure compensation which will minimize image shift during telescope motions. Telescope and star simulators were specially built for this purpose in order to test the optical and mechanical behaviour of the instrument on the 8m-telescope. Acceptance tests of the optical performance and the subsystem tests of all electromechanical functions indicate an excellent quality, especially for the complex Multi Object Spectroscopy unit, while the overall system tests are just starting.

Keywords: optical instrumentation, focal reducer, low-dispersion spectrograph, polarimetry, performance tests

1. OVERVIEW

The two FORS instruments are designed as all-dioptric focal reducers for the ESO Very Large Telescope. They will be capable of doing[1,2]

- direct imaging
- long slit grism spectroscopy
- multi object grism spectroscopy
- polarimetry (FORS1)
- medium dispersion echelle grism spectroscopy (FORS2)

and all sensible combinations of these modes (e.g. imaging- or spectropolarimetry) in the wavelength range from 330 nm to 1100 nm at two angular resolutions (see sections 2.1 and 3.3 below). After a contract signature between ESO and the VIC Consortium consisting of the observatories of Heidelberg, Göttingen and München (December 1991), a preliminary Design Review in April 1992 and a distributed Final Design Review the project is now (1996) in the manufacturing phase with the hardware of FORS1 mostly finished, component and subsystem tests in progress and system tests in preparation. Instrument software is being coded and data reduction software is nearly finished. FORS2 hardware procurement is approximately 80% finished; production and integration will start as soon as FORS1 is freeing the relevant resources. First light of the two instruments is foreseen for late 1998 (FORS1 on VLT Unit Telescope 1) and 2000 (FORS2 on Unit Telescope 3).

2. OPTICAL SUBSYSTEM TESTS

2.1. Imaging optics

The imaging optics of the FORS focal reducers/low dispersion spectrographs are designed to correct for the astigmatism and the residual coma present at the Cassegrain focus of a unit telescope of the ESO VLT as well as for the curvature of the CCD detector itself. Two imaging scales will be offered by the instrument, 0.2 arcsec/pixel in the standard spatial resolution mode and 0.1 arcsec/pixel in the high resolution mode to fully exploit periods of exceptionally good seeing. The image quality of the optical train is tested on the optical bench of the laboratory with a pinhole diameter corresponding to $0.02''$. Table 1 summarizes the calculated and the measured values in image quality on the optical axis; measurements in the field cannot be done in the laboratory since the optical aberrations of the telescope cannot be reproduced there with reasonable effort. Insensitivity of the test CCD in the ultraviolet did not allow measurements in the U filter band. The measured transmission of both instrument optics in both standard and high resolution modes is given in figure 1.

	Standard Resolution		High Resolution	
Filter	Design (80%)	Measured (FWHM)	Design (80%)	Measured (FWHM)
B	$0.06''$	$0.04''$	$0.01''$	$0.02''$
V	$0.05''$	$0.04''$	$0.03''$	$0.03''$
R	$0.06''$	$0.05''$	$0.03''$	$0.03''$
I	$0.07''$	$0.05''$	$0.04''$	$0.03''$
Z	$0.10''$	$0.06''$	$0.05''$	$0.04''$

Table 1: On-axis image quality of the FORS optics as designed and measured on the optical bench. The optics of FORS1 and FORS2 are identical within the accuracy of the measurements.

2.2. Polarizing optics

FORS1 will be for a long time the only instrument at the VLT which allows polarimetric observations at visible wavelengths. It will therefore be equipped with polarizing optics comprising one Wollaston prism and two mosaics for phase retardation. The individual phase retarder plates, each 45×45 mm^2, are of superachromatic (Serkowski) type and assembled in 3×3 mosaics forming a phase plate of 138 mm free diameter. The fast axes of the individual plates had to be aligned by the manufacturer to meet the specification ($\pm 0.1°$) in order to keep the depolarization of the incoming light small. Figures 2 and 3 give the measured phase retardation as well as the effective crystal axis directions for the individual $\lambda/2$ and $\lambda/4$ plates. The image quality of the assembled retarder plate mosaics due to the wedges of the individual plates is better than 80% within one pixel.

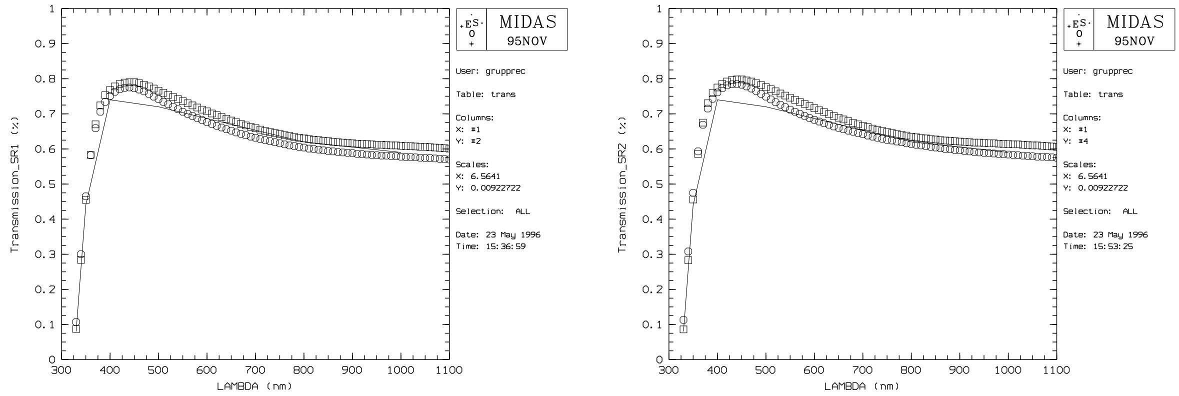

Figure 1: Measured transmission curves of FORS1 (left) and FORS2 (right) optics. Squares: high resolution optics; circles: standard resolution optics; continuous line: specification

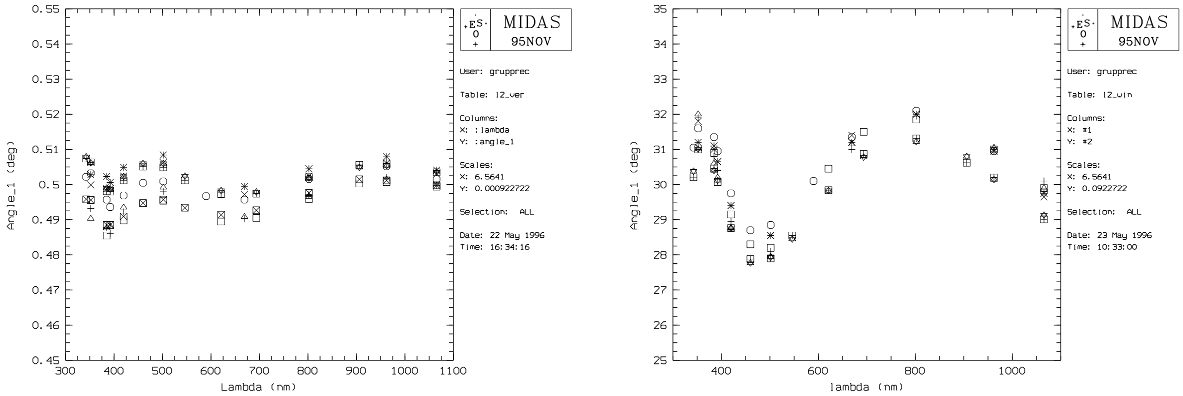

Figure 2: Measured phase retardation (left) and crystal axis directions (right) of the individual $\lambda/2$-plates as function of wavelength.

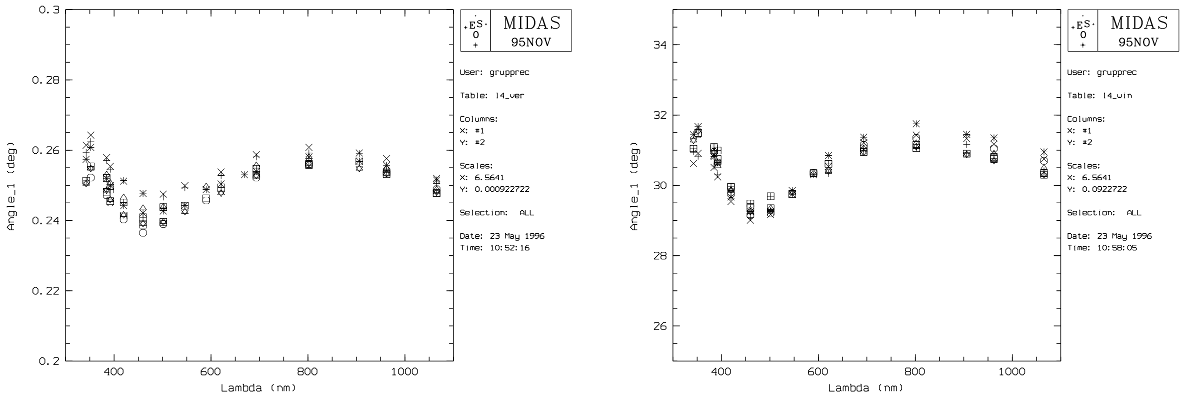

Figure 3: Measured phase retardation (left) and crystal axis directions (right) of the individual $\lambda/4$-plates as function of wavelength.

The Wollaston prism of 132 mm diameter has also been tested; its polarization efficiency is better than 99.99%, its transmission is better than 90% from 350–1100 nm with a peak of 95% at 500 nm, the transmitted wavefront aberration is less than $\lambda/4$. Figure 4 shows the measured beam separation as a function of wavelength. The straight line gives the specification at 632.8 nm ($33.65' \pm 0.1'$).

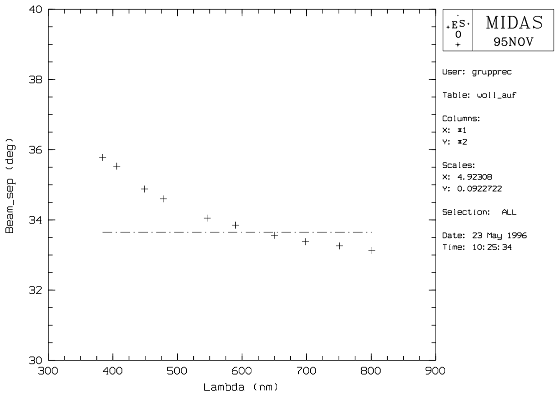

Figure 4: Measured beam separation of the Wollaston prism as a function of wavelength. Dot-dashed line: specification at 632.8 nm.

2.3. Dispersing optics

The FORS instruments will be equipped with sets of at least 7 grisms each with reciprocal linear dispersions between 228 and 44 Å/mm. It will be possible to reach 2-pixel resolution of up to 4400. The grisms are now being manufactured and will be tested next on the optical bench to characterize their efficiencies, spectral resolution and ghost intensity. The prism blanks have passed the in-house acceptance tests meeting the very high quality standards regarding homogeneity (transmitted wavefront error $< \lambda/4$) and transmission (better than the published catalogue values).

3. MECHANICAL SUBSYSTEM TESTS

3.1. Top section

The top section of FORS (figure 5) houses all focal plane devices, the calibration unit and the entrance shutter of the instrument. For object masking within the focal plane of the telescope, three units are provided:

1. the Multi Object Spectroscopy (MOS) unit,
2. a separate longslit unit,
3. an additional (polarization) masking unit.

The most versatile MOS unit supports high quality and simultaneous spectroscopy of up to 19 objects (see section 3.2). In order to have a very clean slit profile for longslit spectroscopy, a separate longslit mask is available providing up to 9 longslits of different widths. Slit selection is done by a decker module. The mask for the standard imaging- and spectropolarimetry will be generated by the slitlet carriers of the MOS unit. An additional mask unit was incorporated to allow for polarization measurements with the high resolution collimator. All masks including the MOS unit will have a cylindrically curved surface in order to adapt them as closely as possible to the spherical focal plane of the telescope. All moving functions of the top section were satisfactorily tested on the subsystem level.

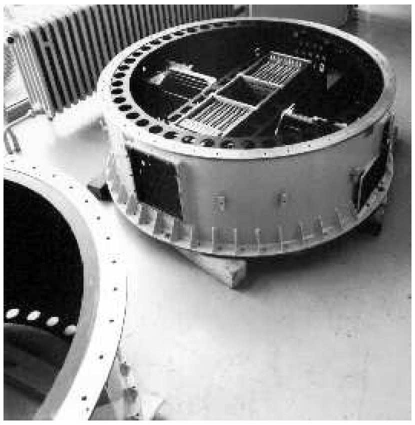

Figure 5: The FORS top section with the MOS unit and the longslit and polarization mask units

3.2. MOS Unit

The MOS unit is a central and the most complex part of the FORS instruments[3]. It provides 19 individual slits each of 22.5 arcsec length. All slitlets can be positioned simultaneously with high accuracy and flexibility. Each slit jaw is individually driven by a high precision spindle in conjunction with an incremental encoder and a DC motor. Motors and encoders are contained in single drive modules which are mounted outside of the housing to provide good accessibility and to minimize heat release inside the instrument. The quality of the linear guides is tested to have a maximum deviation of 3 μm/300 mm length. The quality of the high precision ball-spindles is of the same order and is certified to a linearity of better than 6 μm/300 mm length.

The MOS unit was tested separately from the instrument on a 2-axis movable stand for its performance regarding flexure and positioning accuracy (figure 6). The flexure of the slitlet carriers is estimated to be typically $\pm$25 arcsec for maximum zenith distances of 60° (the operational limit of FORS with full performance). Flexure due to gravity leads to a non-parallelism of the slit jaws of about $\pm$1.5 μm. Some dependence on the field position is observed. Regarding the positioning accuracy, a relative accuracy of about 3 μm on the scale of millimeters could be achieved which corresponds to $\approx 6 \times 10^{-3}$ arcsec and is therefore negligible. A re-positioning accuracy of 0.5 μm could be established which reveals mainly the resolution of the incremental encoders. All other electro-mechanical aspects (like backlash, self-locking, power consumption) are also tested satisfactorily.

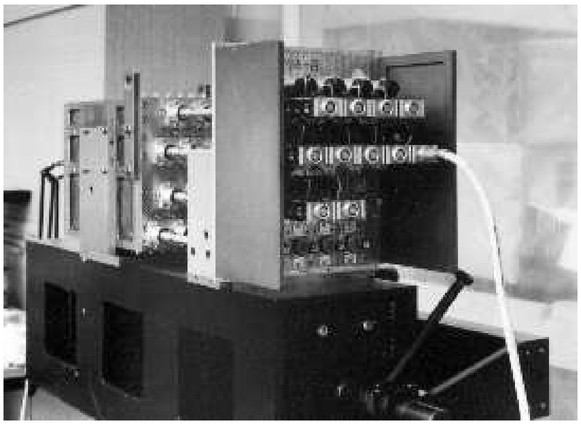

Figure 6: MOS test setup showing the movable support stand on top of which one half of the MOS unit is fixed together with the drive unit containing the 19 individual drive modules.

3.3. Collimator section

The collimator section contains two collimators of different focal length. Each collimator is designed to adapt the image to the pixel size of the CCD detector for different seeing conditions. One collimator ("standard resolution") reduces the image scale to 0.2 arcsec/pixel i.e. suitable for seeing of 0.5 arcsec. The second collimator with twice the focal length ("high resolution") produces an image scale of 0.1 arcsec/pixel and will be inserted into the instrument beam during the periods of exceptionally good seeing. Both collimators rest in a carriage which is mounted between two linear guides in order to exchange the entire optics in the light beam. The lateral motion is limited by hard points which ensure a stable and reproducible positioning in the light path.

The structural stiffness of this exchange mechanism could not yet be tested due to the lack of a reference for measuring this 1.2 m size structure. This test will be performed in the coming phase at the telescope simulator. The best way to estimate the amount of collimator lateral shift is to measure it with the camera itself since the collimator drift will be influenced by the camera unit and vice versa.

3.4. Filter section

The filter section houses the pupil stop and four exchange mechanisms (3 wheels, 1 wheel segment) with the analyzing optics. The first wheel holds the Wollaston prism, cross-disperser grisms and optionally broadband filters, the second wheel the grisms and the third wheel the standard broadband filters. The wheel segment swings the $\lambda/4$ and $\lambda/2$ retarder plate mosaics into the beam. All wheels are worm gear driven rotary stages.

The stability of the wheels and their supports is measured relative to the housing (figure 7) at the 20 μm level. The resulting tilt of the analyzing optics within the beam is by a factor of 10 below the specified value. The positioning accuracy (without backlash in the pre-loaded drive system) is established to the order of $\pm$ 0.5 μm which is basically the encoder resolution.

Power consumption and the time required for positioning all items is also checked in general with the original hardware. All components (except the collimators) can be positioned within about 15 seconds. This allows the FORS instruments the capability of setting up an entirely new configuration in less than half a minute.

Figure 7: Filter/Camera section resting in its turning device that was used in changing the orientation of the part in order to simulate different loads on the housing and the wheels.

3.5. Camera section

The camera section provides five main functions:

1. camera focusing mechanism,
2. interference filter inserts,
3. camera exposure shutter,
4. CCD cryostat interface flange,
5. flexure compensation of the collimator's lateral motion by a corresponding tilt of the camera optics.

The camera focusing compensates for both, temperature variations as well as for different thickness of the interference (IF) filters which will be inserted in the converging beam of the camera next to the CCD entrance window. The insertion of the IF filters separates the camera optics (entrance and exit lenses) which requires a huge focusing range of 12 mm and raises stability problems; however, the advantage is that the transmission characteristics of the narrow-band filters become nearly field independent. Focusing is done by an excenter wheel driving a linear motion stage.

The guiding quality of the three linear ball bearings of the camera focusing mechanism is of the order of 0.8 arcsec for a stroke of 12 mm along which the camera can be focussed with an accuracy of 1 μm. Flexure of the focusing structure which becomes crucial for the passive compensation of the collimator shift is measured to be within $\pm$ 1.5 arcsec. This value corresponds well with the finite element analysis and was thus one of the first proofs of the quality of our finite element model. Further measurements on the deformations of the housing and structures reveal a reasonable agreement with the values determined by the computer model.

The interference filter wheels are tested regarding their reproducibility in positioning with the spur gear drive and a notch. The accuracy which is of the order of 10 μm fully satisfies the requirements.

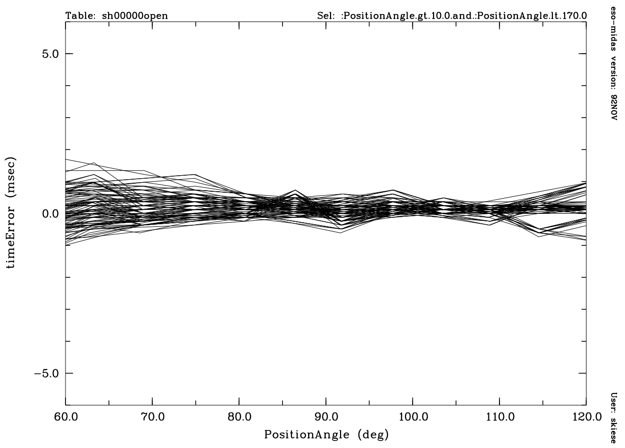

Figure 8: Result of the exposure shutter performance tests showing the deviation from linearity of exposure time in dependence of the field after 360 000 exposures. Over the area of the CCD the uncertainty in opening or closing time is less than 1 msec.

One further crucial part in this instrument section regarding accuracy and reliability is the camera exposure shutter. A new belt driven rotating shutter was developed and a prototype tested. The performance of this device revealed minimum exposure times of 250 msec with a photometric accuracy of better than $\pm$1 msec (see figure 8). The exposure time becomes fully independent of the field at this location, next to the cryostat entrance window, by rotating the sector unidirectionally.

4. TELESCOPE AND STAR SIMULATOR

4.1. Simulator description

In order to simulate the different pointing, slewing and rotational motions of the VLT unit telescope, a dedicated telescope simulator (figure 9) together with two star simulators was designed and manufactured by the FORS Consortium. The telescope simulator provides a two-axis motion i.e. elevation and position angle. It will simulate the telescope motions as closely as possible. Therefore, the load capacity of up to 2.5 metric tons corresponds to that of the VLT telescope at the Cassegrain focus as well as the size and the height of the Cassegrain flange above the floor. Its flange rotation is unlimited whereas in elevation it can point to both horizons. The telescope simulator offers a maximum rotational speed of 100°/min around both axes; this will be controlled in closed loop by a programme or will be operated manually. Remote operation via a serial link (RS232) is also possible.

The two star simulators illuminate the focal plane of the instrument with point sources of appropriate size. One simulator will be used to verify the optical quality of the instrument over the entire field of view in the various observing modes and configurations and at all operating zenith distances. The illumination will provide sources for all purposes of testing the different imaging, spectroscopy and polarimetric modes as well as for calibration. The other star simulator is specially designed for the verification of the passive flexure compensation under various load conditions.

Figure 9: The telescope simulator with a height of approximately 4 m and a base frame of 3×5 m during assembly in the hall with its two support stands fixing the elevation axis to the center of mass of the elevation frame including the FORS instrument. The elevation frame with the rotating Cassegrain flange can also be seen.

4.2. Planned system tests at the simulator

The above simulators will be used in the upcoming project phase to test the fully assembled instrument concerning optical quality as well as electro- and opto-mechanical behaviour. Those system tests will be performed in two stages:

1. functional test under software control in order to verify the electronic control and the software on system level,
2. full instrument test on the telescope simulator including a test and demonstration of all procedures necessary to handle and maintain the instrument.

This second group of instrument tests comprises verification of image quality and scale, field of view, straylight, ghosts and skylight concentration as well as spectral resolution and polarimetric accuracy. For the electronic components, the overall functionality, thermal monitoring and EMC compatibility will be tested and verified. A lot of effort will be spent in testing the mechanical behaviour under different conditions of gravitational load. That comprises measuring the image drift during an exposure and verification of the calculated flexure compensation which works fully passive. The instrumental mass, torque and momentum will be verified in the specified limits. All 52 moving functions of the instrument (i.e. 38 of the MOS unit and all the wheels or exchange mechanisms) will be tested regarding their positioning accuracy, setting time and long term performance. Also the slit quality, slit centering accuracy and slit geometry of the MOS and of the longslit unit will be verified as well as the quality of the focusing and shutter mechanisms. Furthermore it will be shown at the telescope simulator that the FORS instruments can be handled and maintained in an appropriate way with the transport carriage and the tools provided, using the foreseen procedures.

5. ACKNOWLEDGMENTS

We thank all FORS Team members in the Consortium and at ESO who put a lot of hard work into getting a well working instrument. The project is performed under ESO contract 37548/ESO/VLT/91/7844/GWI and is supported by the German Federal Ministry of Education, Science, Research and Technology with grants 05 3GO10A, 05 3HD50A and 05 3MU104.

6. REFERENCES

[1] H. Böhnhardt, S. Möhler, H.-J. Hess, S. Kiesewetter, H. Nicklas, “Design Benchmarks of the FORS Instrument for the ESO VLT”, in: ‘Scientific and Engineering Frontiers of the 8-10m Telescopes’ Tokyo (1994), M. Iye and T. Nishimura, Editors (1995), p. 199

[2] W. Seifert, W. Mitsch, H. Nicklas, G. Rupprecht, “FORS - a workhorse instrument for the ESO VLT” in: ‘Instrumentation in Astronomy VIII’, David L. Crawford, Eric R. Crain, Editors, SPIE Proc. 2198,213(1994)

[3] W. Mitsch, G. Rupprecht, W. Seifert, H. Nicklas, S. Kiesewetter, “Versatile multi object spectroscopy with FORS at the ESO Very Large Telescope” in: ‘Instrumentation in Astronomy VIII’, David L. Crawford, Eric R. Crain, Editors, SPIE Proc. 2198,317(1994)